Journal of Innovative Materials in Extreme Conditions
2023
Volume 4
Issue 2

THIN FILMS AND MONOLAYERS – PREDICTION, MODELING, AND EXPERIMENTS

J. Christian Schön[1,*], Dieter Fischer[1]

[1]Max Planck Institute for Solid State Research, D-70569 Stuttgart, Germany
Corresponding author: C.Schoen@fkf.mpg.de*

Abstract: *The development of new materials in an efficient fashion requires progress both in the computational search for promising targets and in the design of suitable synthesis routes by a combined effort of theory and experiment. This applies not only to bulk materials but also to low-dimensional systems such as thin films and monolayers. In this presentation, we will discuss some of the methodological features specific to the prediction and synthesis of (meta)stable (quasi)-low-dimensional systems, together with examples of structure prediction and modeling for crystalline and amorphous atom- and molecule-based monolayers and thin films. This is complemented by direct comparisons with experiments, and the discussion of additional thin film experiments that focus on new structural insights in seemingly completely understood systems like gallium and ZnO films.*

1. Introduction

New chemical materials and compounds serve as the foundation for the modern technology of our civilization, where these materials should be environmentally friendly, with stable and controllable properties for a multitude of applications, and at the same time energy efficient in their synthesis as well as easily recyclable.[1,2] In particular, the development of new devices, of ever greater sophistication yet smaller size at the same time, requires providing new types of inorganic or hybrid materials, whose structure can be controlled down to the atomic level, in order to fine-tune their physical, and chemical and/or biological properties.[3-5] Traditionally, such materials are generated in bulk and then chemically machined down to whatever size is needed.[6,7] But such materials are also often grown in a bottom-up approach on a substrate, and in the extreme, we are dealing with and aiming for low-dimensional systems with bespoke properties, where details of their structure and the stability of such materials often become an issue of concern.[8,9]

The ability to predict such (meta)stable nanomaterials via the investigation of their energy landscapes, followed by a computation of their properties and stability, is of great value in their design and synthesis.[10] Over the past three decades, the structure prediction of 3D bulk crystalline compounds, atom clusters, and (bio)molecules has shown great progress,[11-13] and the computational approaches used are expected to be also applicable to low-dimensional systems.[14] Such landscape explorations are of great value since the synthesis and design - within the limitations of physical laws - of such materials often lead to compounds or modifications that are metastable or only stable under certain specific structural or thermodynamic boundary conditions. Thus, further insights come from modeling and simulating the synthesis process, and the detailed experimental study of the structure and properties of these materials.

Furthermore, since we are not necessarily dealing with macroscopic bulk phases that are thermodynamically stable, the outcome will be greatly influenced by the details of the synthesis route. But trying to design a path to a desired compound, whose structure is controlled on the atomic level, is only possible if we know the many feasible (meta)stable phases, as a function of the thermodynamic and process parameters, that might appear along the road as intermediary modifications or even constitute traps to be avoided. Conversely, studying the energy landscape of the system, on which these modifications are located, allows us to identify promising targets for such a synthesis, especially if they are predicted to exhibit useful properties.

Besides such targets and competing phases, a full design of a synthesis route requires information about the evolution of the structures on both the atomic and the mesoscopic levels. Both reliable comprehensive experimental data and extensive input from theory are needed to provide this information about the processes involved. [15] Once such descriptions are available, optimal control

methods can be applied to identify the choice of an (optimal) synthesis route or the optimal schedule of the parameters for a given type of route [16-18], yielding the desired outcome.

The theoretical tools as such are well-known - molecular dynamics and Monte-Carlo simulations or through global explorations of the energy landscape on the one hand and in the form of differential equations representing, e.g., reaction-diffusion and various growth laws on the other hand, thus describing the evolution of the system on the atomic and mesoscopic level, respectively - although need to be adjusted for every chemical system and proposed synthesis route, and encounter obvious limitations due to numbers of atoms involved and the computational cost of the energy and force calculations when performed on the ab initio level. In contrast, sufficient input from the experiment is usually lacking in the case of solid-state synthesis. The reason for this is a "psychological" one, due to the historical focus on describing the one synthesis route that yielded the new never-before-seen compound. However, in order to provide the necessary information for modeling and optimizing a synthesis route, one needs not only a careful analysis of the specific synthesis route (including the associated parameters) that has been successful in producing the desired compound but also analogous detailed information about the outcome of unsuccessful routes or parameter choices for the synthesis of this specific compound! This includes, e.g., which byproducts have been produced, what parameter choice increases the yield, what influence certain impurities have, etc., ideally not only at the end but also along the various stages of the different synthesis routes and studied parameter schedules.

While such information is often available for organic syntheses, for inorganic compounds such data are commonly lacking or, if available, have not been published, since the focus of the solid-state chemist and materials scientist usually is on the "successful" synthesis of a new compound and not on the analysis of the synthesis route as such. One reason for this is the very time-consuming investigation of all the parameters involved in the synthesis. But such data are highly valuable, since they greatly increase our knowledge of the chemical system itself, allow the formulation of general laws effectively describing solid-state syntheses, and would be expected to be transferable, with slight modifications, to other chemical systems, for which successful syntheses are still lacking, especially in combination with theoretical analyses of the system and the attempted synthesis routes.

This issue will take on an even greater urgency as the availability of sufficient computer resources and general expertise in machine learning [19,20] will allow us to attempt to train large neural networks to predict the outcome of proposed synthesis routes for achieving a given chemical systems - or even directly suggest the best route for a given target compound or modification. In a way, this would be the computer science equivalent of incorporating the knowledge of many experienced experimental chemists into the "ideal wise chemist". However implementing this approach will require the availability, as input, of a plethora of detailed information about both the successful syntheses and those which have "failed" to produce the desired outcome.

Another related issue is often the lack of full and detailed information about the structures of the synthesized compounds of interest, ideally as a function of the synthesis route. Due to the overwhelming pressure to generate new compounds with exciting new properties, one frequently observes that the structures of the published compounds are known only in quite a rough fashion - if at all -, where reflections in diffraction patterns, bands in Raman or IR spectra, UV-VIS measurements, etc., are not fully explained or just attributed to some unspecified disorder in the system. Here, theory can only assist by pointing out that these peaks should not appear in the data assuming that the compound exhibits the proposed "ideal" structure. But theory by itself cannot identify, in a definitive way, where to look for explanations, unless we can fully model the whole synthesis starting from the educts and taking all admixtures or surfaces of reactions, etc., into account. Clearly, clarifying such issues and identifying the underlying structural peculiarities of the material is an important challenge that needs to be answered by the experimentalist.

However, although these subtle quasi-invisible features can influence the properties of a material to a large extent, it is not easy to extract such information for macroscopic 3D-bulk systems. Besides explaining the physical properties of a given material, we need to address even more fundamental questions regarding our control of a chemical system: Can we specifically synthesize all polymorphic forms of a compound? Do we understand which differences in synthesis procedures and choices of synthesis parameters are responsible for the formation of these different crystal structures? But such detailed information can often be obtained, and much control over the synthesis is expected,

if the system is of lower dimension. Examples of such systems are two-dimensional monolayers of atoms or molecules, either free-standing or on a substrate, and thin films that have been deposited from a gas phase of controlled composition without impurities in high vacuum at low temperatures, thus avoiding the complication of the presence of a solvent or flux and the high temperatures and pressures often used in solid-state syntheses.

The amount of work that has been done on such thin films and monolayers is enormous and doing it justice in a comprehensive fashion would result in a large review far beyond the purview of this contribution.[21,22] Instead, we will present some prototypical examples drawn from our work, which illustrate the issues and challenges mentioned above.

2. Methods

In order to avoid getting into technical details in the example section, we are summarizing the methods - theoretical and experimental ones - that have been applied in the examples presented below. For more details on the algorithms and synthesis methods mentioned, we refer to the literature and the original publications.

2.1. Theory

In the examples below, a variety of computational methods have been employed. To start with, global optimizations have been performed on the energy landscape of the chemical systems, in order to predict the structure of molecules and atom clusters in vacuum and on surfaces, to predict the arrangement of monolayers of atoms and molecules on a substrate or as a free-standing 2D-monolayer, and to predict the structure of bulk crystalline modifications in 3D. The algorithms employed have been simulated annealing (SA) [23], both with and without large jumpmoves - sometimes combined with local minimizations directly after the jumpmove -, the threshold algorithm (TA) [24,25] and the closely related threshold minimization (TM) algorithm [26], and the IGLOO algorithm [27].

All of these are stochastic optimization and energy landscape exploration algorithms that are based on random Monte Carlo (MC) walks in configuration space employing both simple and complex moveclasses, with or without a prescribed energy threshold, and often combined with periodic local optimizations. These are performed at different temperatures: $T = 0$ K (stochastic quench where only downhill steps are accepted), $T = \infty$ (unbiased random walk where every step is accepted), and $0 < T < \infty$ (every step is accepted according to the Metropolis criterion [28]).

Next, molecular dynamics (MD) simulations have been employed for modeling monolayers of molecules and atoms and their evolution with time, for the simulation of the deposition processes and growth of thin films, and for the computation of properties such as diffusion constants or the phonon density of states. We note that the global optimizations and MD simulations are usually performed with robust generic or specially adapted empirical potentials, but in some cases, ab initio energies were employed.

All promising structure candidates obtained during the global optimization were locally optimized on ab initio level. For those 3D crystalline modifications with low energies, the energy was also computed as a function of volume, or the enthalpy as a function of pressure, respectively, in order to be able to estimate, which ones would be classified as standard pressure, high pressure or effective negative pressure phases.

Finally, various properties were computed, on ab initio level, such as band gaps, Raman spectra of clusters or of crystalline modifications - with and without defects -, in order to interpret the peaks in the experimental data of molecules/clusters in the gas phase and of the thin films that exhibit nucleation and growth of crystalline phases.

2.2. Experiments

For the study of single non-reactive molecules and monolayers thereof on a metal substrate with smooth surfaces, the electrospray ionization (ESI) method was employed [29], while for the deposition of precursor molecules that react to form periodic or amorphous monolayers on a substrate, the gas phase resulted from sublimation of the precursor molecules. The thin films were generated using the low-rate/low-temperature deposition technique, which works on the border of the beginning of crystallization. Here, a beam of atoms and/or few-atom cluster fragments was generated by thermal evaporation [30] or via pulsed laser ablation [31] of materials with the same composition as the thin film that should be grown. In special cases, the electron beam gun evaporation combined with a plasma activation of gases was used [32,33]. The deposition usually takes place at reduced mobility conditions (low deposition temperatures T_D between -240 °C and + 450 °C) which allows the local addition of individual atoms or cluster fragments on the atomic level without large atom movement on the surface, thus forming a homogeneous, originally amorphous, deposit. Thus, a large variety of (meta)stable phases can readily nucleate and grow even when one tempers at quite low temperatures, and subsequently transform into other modifications upon slow heating and cooling of the deposit.

3. Examples

In this section, we will present a number of prototypical examples that illustrate a variety of aspects of the modern view of syntheses, ranging from structure prediction of target compounds to complete synthesis modeling as far as theory is concerned. Regarding the experiments, they deal with the deposition of monolayers via the gas phase and the systematic analysis of phase formation and transformation as a function of synthesis and subsequent treatment parameters for thin films in the experiment. These investigations are moreover combined with a detailed analysis of the generated phases and their properties as a function of the deposition parameters.

3.1. Prediction of 2D monolayers in the Si/C system

Monolayer graphene being a material with exciting properties, it is a natural question to ask, how the admixture of Si atoms would affect its behavior. Since only (meta)stable compounds should be considered for such a hypothetical material, in the first step, the energy landscape of Si_xC_{1-x} two-dimensional structures was globally explored for a range of values of x (x = 1/4, 1/3, 1/2, 2/3, 3/4).[10,34] For each choice of x, the global minimum consisted of a graphene-analogue structure, where a fraction x of the carbon atoms in graphene were replaced by Si atoms; however, many other network structures consisting of a mixture of rings of three, four, five, six, seven, eight or more atoms, were also frequently found as kinetically stable structures. Since there is no efficient robust empirical potential for the Si/C system, the global optimizations using the SA algorithm with jumpmoves were performed on ab initio level (DFT).

When comparing the energy of these configurations with the energy of decomposition into a fraction (1-x) of pure C-graphene and fraction x of pure Si-graphene, only the alternating (see Figure 1) graphene analog with composition Si : C = 1:1 was thermodynamically stable [34]. Considering the band structures of Si-, C-, and SiC-graphene, we find that those of C-graphene and Si-graphene are very similar with both exhibiting Dirac points, while the SiC-graphene structure is a semiconductor with a finite band gap of about 2.5 eV.

We note that recently, Polley et al. [35] have succeeded in preparing the alternating SiC-graphene analog by first depositing an ultrathin transition metal carbide film (TaC) on a silicon carbide substrate. Then the system was slightly heated such that Si and C atoms of the substrate diffused in equal amounts onto the TaC surface, and with Si and C atoms being in close proximity to each other, a monolayer of SiC-graphene could form as the "nearest" thermodynamically stable minimum.

This example nicely demonstrates the successful application of suitably modified versions of the well-established crystal structure prediction methods to low-dimensional systems, with a subsequent realization of the predicted structure in the experiment. However, it also demonstrates that the successful synthesis method is not a very straightforward one, at least for the non-expert in thin film and surface layer modification and growth.

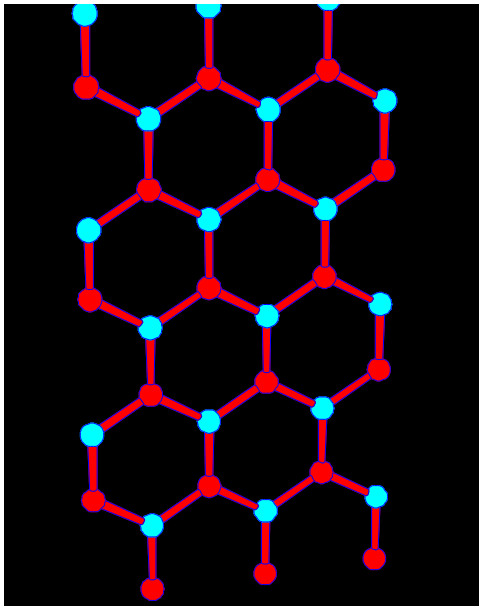

Figure 1. Structure of the global minimum of a monolayer of SiC. Red spheres and blue spheres represent carbon and silicon atoms, respectively.

3.2. Prediction and synthesis of monolayers of sucrose molecules on a Cu(100) substrate

As a second example, we consider the formation of periodic monolayers of sucrose molecules on a Cu(100) surface [36]. From a theoretical point of view, modeling the full synthesis, i.e., the generation of the gas phase via ESI, the deposition of the gas of protonated or deprotonated or otherwise charged sucrose molecules on the surface and the diffusion based re-arrangement of these molecules into possible amorphous and periodic structures would be highly complex and computationally extremely expensive: already the analysis of the deprotonated molecule in a vacuum takes a large effort to describe and analyze because of the many (22) hydrogen atoms that can be involved in the deprotonation [37]. Thus, we have employed global optimization techniques in a stepping stone approach, to obtain structure candidates for the (periodic) sucrose monolayer on the surface for comparison with the experiment.

As a first step, the TM algorithm using an AMBER force field was used to obtain the optimal shape of the neutral sucrose molecule in vacuum [26], where all angles and atom-atom-distances were allowed to vary. Next, this molecule was placed on the metal surface in various orientations as the initial configurations for a second round of global optimizations, where the optimal shape, orientation, and location of the molecule on the metal surface were identified [38], using the IGLOO algorithm. Here, the interaction with the surface was via a Lennard-Jones term and an image charge term, while only a limited number of internal degrees of freedom of the sucrose molecule, the dihedral angles, were allowed to be varied, together with the orientation and location of the molecule with respect to

the atoms in the Cu-surface. The best candidates were locally re-optimized on the ab initio level on the Cu-surface, where all atoms in the molecule were allowed to vary.

The optimal structure of the single molecule on the surface was used as input to the global search for low-energy periodic configurations of the sucrose monolayer, represented by a finite number of sucrose molecules in a variable 2D-periodic simulation cell with the actual Cu-surface being replaced by a featureless metal-like surface. Here, the individual molecules were treated as rigid, but they were allowed to be shifted and rotated in the plane of the surface, together with the variation of the cell parameters of the simulation cell. The result was a very large number of low-energy structures that all corresponded to slightly different compact packings of the sucrose molecules [38] (see Figure 2 for a typical example).

In parallel, the experiments produced STM images, which showed a periodic arrangement of bright and dark regions of sizes on the order of about half a sucrose molecule, with a more or less quadratic arrangement of these elements, suggesting a square-like unit cell.[39] By computing the STM images of the individual sucrose molecules arranging these in a compact fashion analogous to the results of the global optimization, and comparing these arrangements with the experimental STM images, a good agreement between theory and experiment was achieved [36].

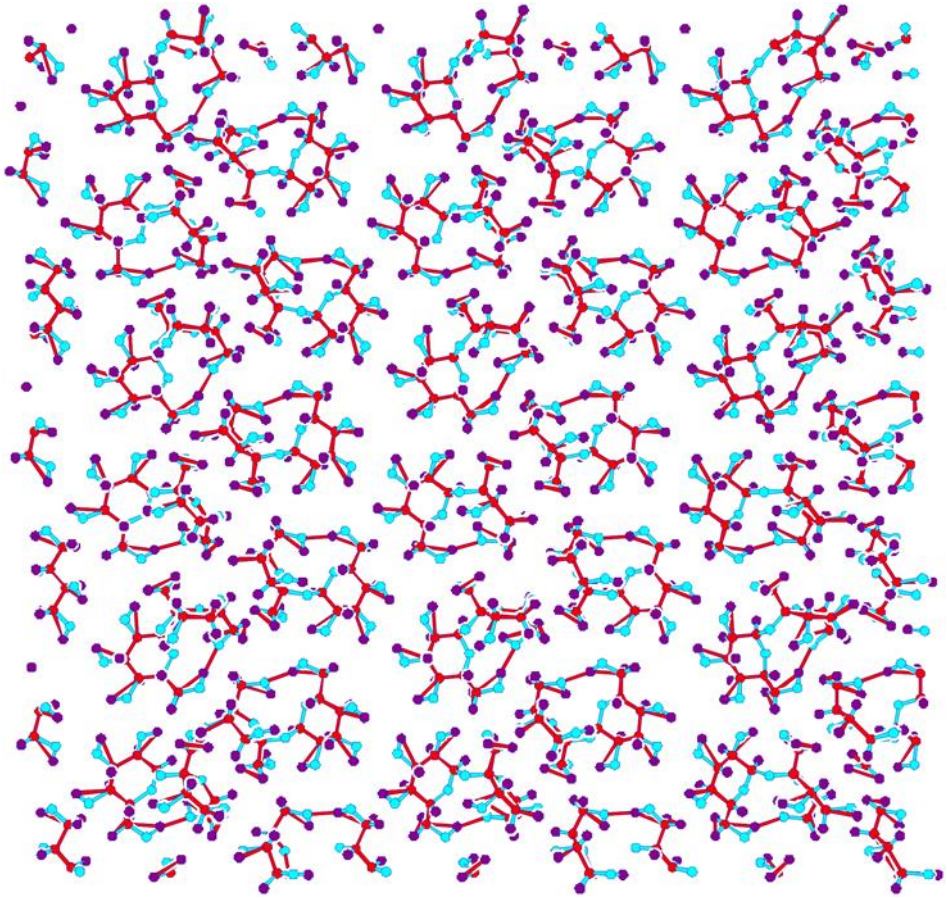

Figure 2. Low-energy local minimum of a monolayer of sucrose molecules, with four molecules in the variable periodically repeated simulation cell. Red, blue, and purple spheres correspond to carbon, oxygen, and hydrogen atoms. Note that each molecule contains 45 atoms, many of which are projected on top of each other in this view along the vertical to the surface.

This study underlines the importance of close collaboration between theory and experiment, in particular, if the system consists of many (large) molecules and surface atoms with a large variety of interaction types involved. In such a case, the number of atoms that need to be taken into account is so large, and in addition, the synthesis process is so complex, that a complete synthesis modeling and

structure prediction on ab initio level is not feasible. As a consequence, the structure prediction needs to take place in stages [38]; however, the gain in "efficiency" is paid for by the price of potentially large inaccuracies when the hand-over between two stages of the modeling process occurs.

3.3. Modeling and synthesis of amorphous monolayers of 1,3,5-tris-(4-bromophenyl)-benzene on an Au(111) substrate

The periodic arrangement of sucrose molecules on the Cu-surface was due to a combination of dense packing - thus maximizing the van-der-Waals interactions among the molecules -, hydrogen bridge bonds, and relatively weak (mostly dipole and quadrupole) electrostatic interactions between the molecules. As a consequence, the molecules could quite easily move about and rearrange themselves within a certain temperature window-, thus achieving energetically optimal (periodic) packings. However, if the temperature was too low, the molecules remained essentially frozen where they were deposited, as could be seen during the analogous deposition of trehalose, where a variety of arrangements of the molecule in small groups of molecules were observed [40], while at higher temperatures the molecules diffused very rapidly on the surface thus preventing the formation of any stable structures visible in the STM. The characteristic features of these packings could be predicted within the limitations of the purely global optimization approach to structure prediction, which typically aims at the structure that has the lowest energy and thus would be guaranteed to be the thermodynamically stable one at a temperature of 0 K. These limitations include imperfect energy functions - even on ab initio level, van-der-Waals and hydrogen-atom mediated bonding are non-trivial to account for -, small energy barriers against molecular re-arrangements combined with a multitude of low-energy arrangements. Adding finite temperatures that allow the molecules to switch between different arrangements, these limitations makes a perfect prediction nearly impossible, although one on the level of the experimental (STM) accuracy - where the resolution is usually not higher than ca. 1/2 nm - is possible.

This contrasts with the case of precursor molecules that react with one another on the surface, usually via reactive functional groups at the rim of the molecule, releasing, e.g., X_2 (X = F, Cl, Br, ...) gas molecules in the process. The resulting network of covalently bound molecules (actually, the remaining molecular cores of the precursor molecules) is thus quite stable, and rearrangements are exponentially slow at temperatures below those at which the molecules themselves decompose or the network degrades. As a consequence, the network largely reflects the original more or less random amorphous arrangement of the precursor molecules, analogous to the case of a network-type glass former like SiO_2 when cooled below the glass transition temperature [41]. Once the network has formed, changes in the frozen-in yet energetically non-optimal structure take place on logarithmically slow time scales, similar to the aging processes in glasses [42-45].

From a theoretical point of view, the appropriate approach thus takes its inspiration from the modeling of the glass transition or precursor-based 3D network formation and the simulation of the evolution of glasses and other amorphous compounds, i.e., one performs very long MC or MD simulations, while including the formation (and subsequent rare breaking) of bonds between the precursor molecules via appropriate empirical potentials.

As an example, we consider the amorphous network of 1,3,5-tris-(4-bromophenyl)-benzene on an Au(111) substrate, where each of the molecules could form three covalent bonds to neighbor molecules in a triangular fashion [46]. The experiment yielded an irregular network of triangular nodes (each representing one of the molecules) with a wide distribution of ring sizes - predominantly ranging from 4 to 8 -, where the optimal arrangement would have been a perfect hexagonal lattice. For the simulations, we performed long-time MD simulations of partly rigid molecules, i.e., the atoms inside each of the four rings consisting of six atoms each, which together constituted the individual molecules, were rigidly connected. The resulting structures (for example, see Figure 3) were very similar to the experiment. They showed good agreement with the experiment regarding both the ring-size distributions and the distribution, overall molecule nodes of the network, of the sets of the possible combinations of the sizes of the three rings that share a common corner molecule. Furthermore, the plot of the average energy of the network vs. the logarithm of simulation time

exhibited a smooth linear decrease over many orders of magnitude as expected from a typical system with standard aging behavior.

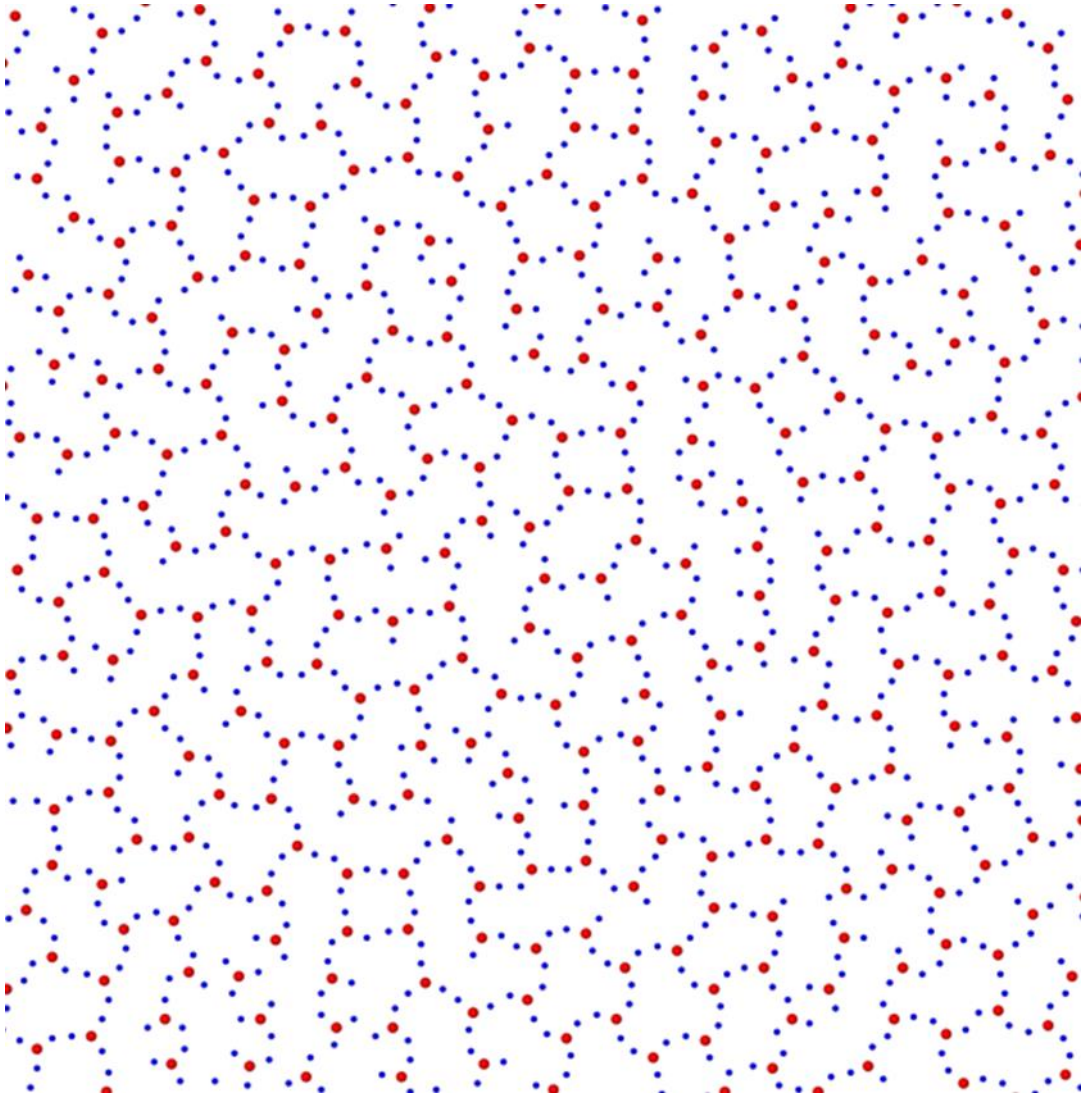

Figure 3. Except from an amorphous two-dimensional network of 1,3,5-tris-(4-bromophenyl)-benzene during a MD simulation of 5750 model molecules. The red and blue dots represent the central benzene and the three bromophenyl groups of the molecules, respectively.

While the modeling did not take into account the atom level processes that occurred during the reactions that formed the covalent bonds between the molecules, it captured the creation and evolution of the network of the molecules in a satisfactory manner. In particular, by changing the parameters in the effective potential describing both the molecule-molecule interactions and the interior flexibility of each molecule, it would be possible to suggest the outcome of the network formation for other (triangular) molecules that interact more weakly or more strongly or exhibit different degrees of internal flexibility, than the original molecular system studied. This would allow us to select a-priori the right kind of molecular building blocks to achieve specific networks (defined by their ring-size distributions) with a high probability and predict their stability as a function of evolution time.

3.4. Prediction of 3D crystalline LiBr modifications and their realization in thin films

Turning to the investigation of thin films, the analysis of LiBr thin films deposited at low temperatures is a classical example of a true 3D crystal structure prediction followed by a successful synthesis of one of the predicted yet previously not observed (meta)stable modifications [47-49]. Using the SA algorithm for global optimization on the empirical potential energy landscape followed by ab initio level local optimizations of the promising structure candidates, the resulting E(V) curves indicated that besides the known rocksalt type modification, a number of other ones, including a wurtzite, sphalerite and 5-5 type [50,51] modification, should be accessible and stable at standard pressure and moderately low temperatures. In fact, depending on the density functional employed, one of the structures with four-fold coordination, such as the wurtzite-, sphalerite-, or the β-BeO-type, might have a lower energy than the known rocksalt-type structure of LiBr.[47,48]

To explore the configuration space experimentally, the low-rate/low-temperature approach was employed using evaporation from a heated LiBr solid as a source to deposit Li/Br atoms and cluster fragments on a sapphire substrate.[49] The deposition rate (characterized by the vapor pressure p_D) was systematically varied ($1 \leq p_D < 8x10^{-4}$ mbar) as well as the temperature of the substrate (typically called the deposition temperature T_D) using a resistance heater (-100 °C $\leq T_D \leq$ 0 °C), and the outcome was carefully recorded (see Figure 4). As a result, an optimal combination of pressure and T_D was determined for which the new predicted wurtzite modification β-LiBr could be obtained in 100% of the syntheses. Furthermore, this study demonstrates the importance of a dense mesh size of the (p_D,T_D) parameter set. In the experiments with T_D below -100 °C, at low vapor pressures amorphous samples were obtained, which transform during heating into the stable rock salt modification, while at higher vapor pressures broad reflections of the rock salt modification directly emerged in the diffraction patterns. Similarly, for depositions above 0 °C the rock salt type is detected, too. However, for T_D between -100 °C and 0 °C, the β-LiBr can be stabilized where the likelihood of obtaining this modification systematically varies as a function of p_D and T_D.

Besides being a very nice example of a true successful prediction with subsequent experimental verification, this case also provides a demonstration of the proper way to not only present a newly synthesized modification but also to perform a quantitative analysis of the outcomes for a large range of the synthesis parameters. We note that an analogous successful validation of prediction was achieved for LiCl, where again the prediction of a wurtzite modification [47,48] was confirmed by the experiment [52].

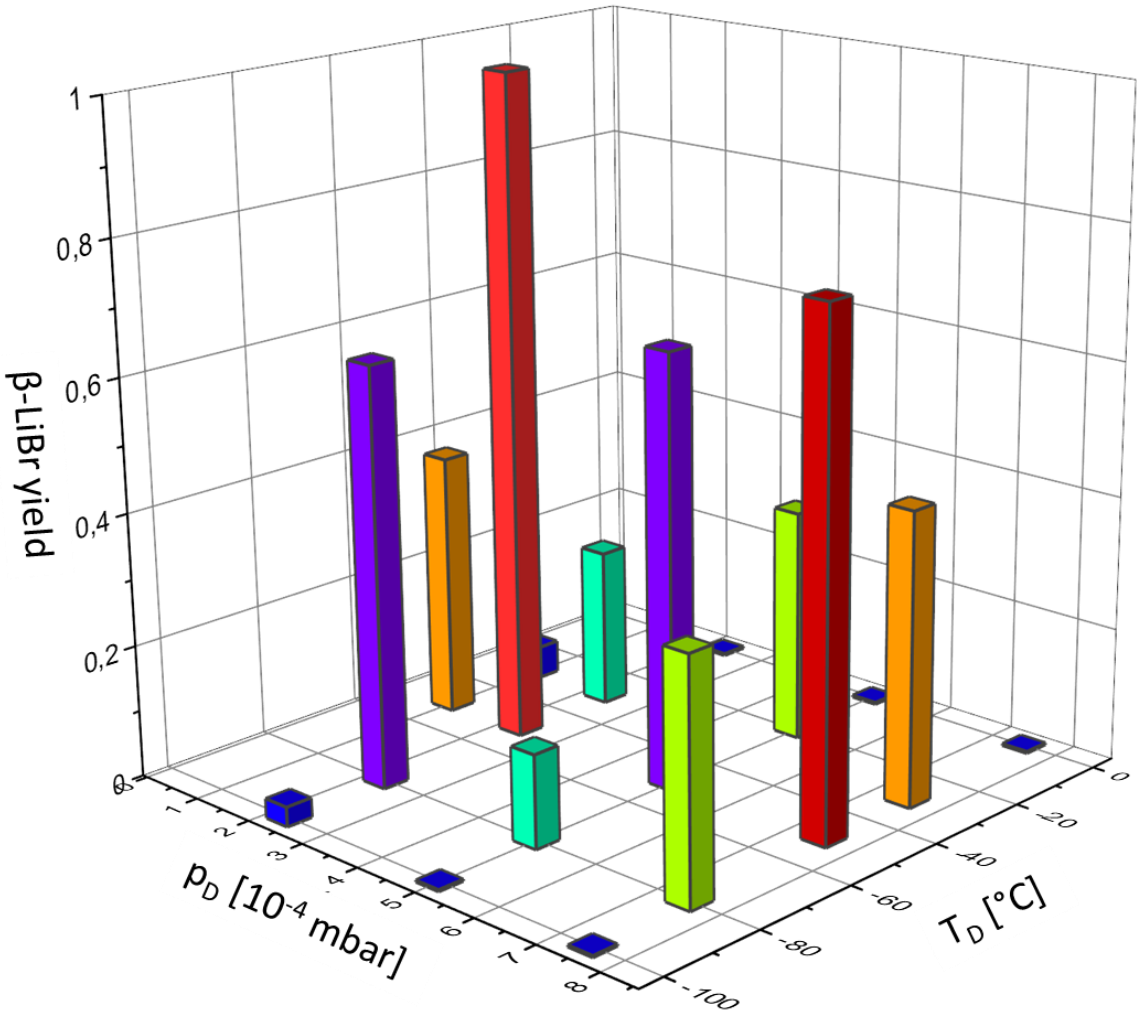

Figure 4. Yield of β-LiBr (wurtzite structure type) as a function of LiBr vapor pressure p_D and substrate temperature T_D for a set of depositions of LiBr on a sapphire substrate.

3.5. Theoretical modeling of the deposition of thin films of MgF_2 on a sapphire substrate and their tempering at elevated temperatures combined with their experimental realization

Considering the great success of the deposition at low temperatures combined with the variation of the deposition rate in generating new compounds or new crystalline modifications of known compounds, the question arises, what is happening during the deposition-annealing process on the atomic level? The fact that several of the first test systems yielded so-called high-temperature phases inside an amorphous film deposited and tempered at temperatures far below those at which the HT-modification is usually synthesized,[32,53] suggests that a competition among nuclei of several different crystalline phases of the compound of interest exists inside the amorphous deposit. These studies require an in-situ characterization of the samples during the annealing process, which was realized by a transfer of the samples from the deposition chamber to the various measurement apparatuses while maintaining cooling and vacuum. To achieve this, a special cart system was employed that allows a suitable transfer of the deposited films as well as of an argon matrix containing embedded gas phase species to an X-ray diffractometer with an integrated Raman spectrometer. Furthermore, the films can also be directly deposited on a TEM sample holder at low

temperatures and subsequently transferred in a vacuum to an electron microscope for in-situ TEM characterizations.

Quite generally, since the density of the deposit is usually lower than the ones of the feasible crystalline modifications, each nucleus of a crystalline phase will have a higher density than the surrounding amorphous material and thus will experience an effective negative pressure due to forces exerted by the atoms in the amorphous phase on those belonging to the "surface" of the nucleus. Thermodynamically, this clearly favors the nuclei with the lowest density, and once such a nucleus has reached a critical size, it can continue to grow even after the direct contact with the enclosing amorphous matrix has been lost thus eliminating the effective negative pressure, and become a kinetically stable though thermodynamically metastable crystal. This argument is also supported by the E(V) curves of the various crystalline modifications, where we can estimate the effective negative pressure at which the low-density modification would become the thermodynamically stable one.

While being a convincing thermodynamic argument and yielding a plausible easily visualized scenario of the processes taking place inside the amorphous film during the tempering stage of the synthesis, it lacks both experimental and theoretical evidence. In particular, since it is not clear at all that the hypothetical nuclei are really nearly spherical enough with a well-defined surface separating them from the atoms belonging to the amorphous phase to allow the establishment of a "real" negative pressure, we need direct atom-level information, either from theory or experiment or both.

Thus, we have investigated the deposition and growth of thin films of MgF_2 on a sapphire substrate at low temperatures to generate the films,[54,55] and complemented this by computer simulations of the complete process [55,56].

Regarding the experiments, depositions were performed at different deposition temperatures ($-228\ °C \leq T_D \leq 450\ °C$) and a variety of vapor pressures, where the gas phase was generated via an effusion cell. Directly after deposition at low temperatures, the deposit was X-ray amorphous, and upon tempering at slowly increasing temperatures, first, a slightly disordered $CaCl_2$-type phase was identified, which at somewhat higher temperatures transformed first into a disordered and finally into a fully ordered rutile phase, which is the well-known modification of MgF_2 at standard pressure.[54]

Regarding the theoretical simulations, we note that ca. 25 years ago, global optimizations with empirical potentials had identified a variety of promising structure candidates for MgF_2 besides the global rutile minimum, such as an anatase-type, a CdI_2-type, or a half-filled rocksalt-structure (reminiscent of an AB_2 analogue of the Li_3N structure but with MgF_6 square bipyramids, i.e., slightly squeezed octahedra, instead of the NLi_8 hexagonal bipyramids).[57,58] While in other analogous AB_2 systems distortions of the rutile structures resembling the $CaCl_2$ structure appeared as local minima for some of the empirical potential parameters [57], for the MgF_2 system relaxations on both the empirical potential and ab initio level had shown that the $CaCl_2$-type structure was kinetically unstable transforming instantaneously into the rutile-type structure, contradicting the claim of the experiment to have observed a $CaCl_2$-type modification in the tempered MgF_2 films.

In order to clarify this issue and to fully reproduce the synthesis of the MgF_2 films, the theoretical modeling proceeded in three stages. First, global optimizations on empirical potential and ab initio level for neutral and charged Mg/F clusters of various compositions including $(MgF_2)_n$ (n = 1,...,10) clusters were performed using SA and TA. [59,60] For many of the small low-energy clusters, Raman spectra were computed and compared with the spectra taken from the gas phase in the experiment, thus identifying both MgF_2 monomer and MgF_2 dimer species, plus some charged molecules, as the dominant components of the gas phase after thermal evaporation.[60]

In the second stage, these clusters were deposited on a cold sapphire substrate at a constant rate, using MD simulations with empirical potentials. This resulted in an amorphous phase that was in good agreement with the experiment, according to the X-ray diffraction data.[55]

In the final stage, the deposit was tempered at elevated temperatures, again using MD, yielding a layered structure of alternating Mg- and F-atom sheets.[56] Upon closer analysis, it was found that the structure consisted of a multitude of small regions that exhibited the $CaCl_2$-type or the CdI_2-type structure (see Figure 5), where these crystalline regions shared all the sheets of F-atoms that extended throughout the film parallel to the xy-plane, i.e., to the surface of the substrate. In general, the $CaCl_2$-type regions were larger than the CdI_2-type regions, though both were clearly identifiable.

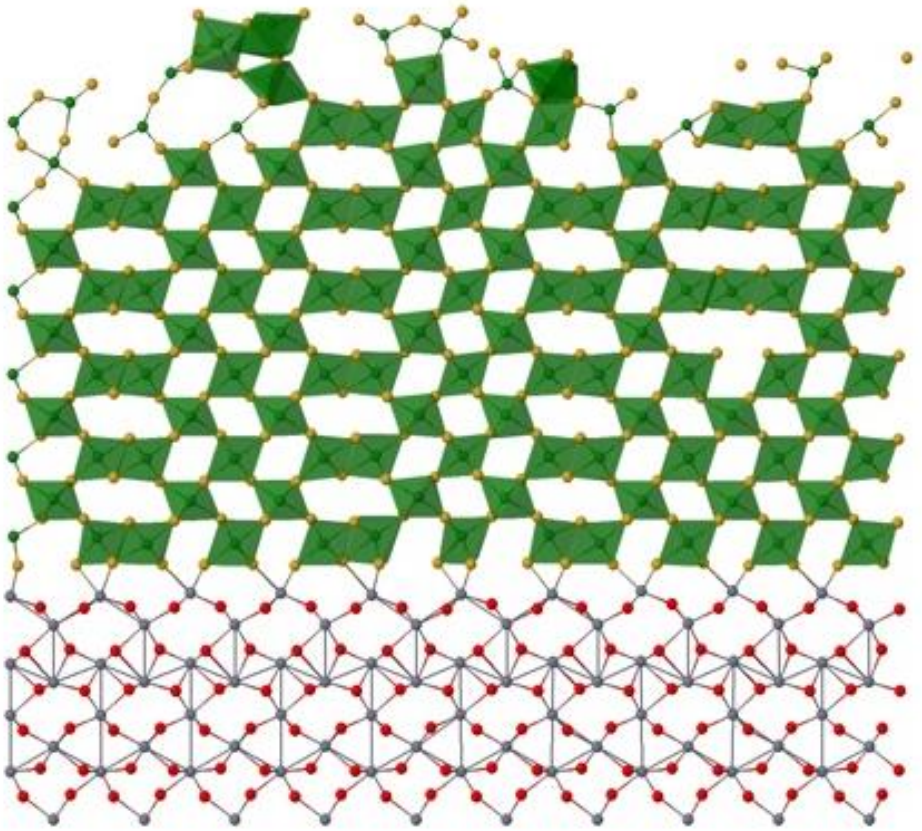

Figure 5. Outcome of a typical simulation of the deposition and annealing of MgF_2 on Al_2O_3 substrate. The substrate was kept at T_D = 50 K during the deposition, and the deposit was subsequently annealed for 3 ns at 1500 K. Al, O, Mg, and F atoms are shown as grey, red, green, and golden spheres, respectively. In order to allow easier visualization of the nano-size regions of crystallites of the $CaCl_2$- and CdI_2-type, we also depict the MgF_6 coordination polyhedra as semi-transparent slightly distorted green octahedra. (Reprinted with permission from S. Neelamraju, J. C. Schön, M. Jansen, Inorg. Chem., (2015), 54, 782-791; Copyright 2015 American Chemical Society.)

In the case of the CdI_2-type regions, only every second layer between the F-sheets was filled with Mg-atoms, as expected for a CdI_2-type structure. In contrast, in the $CaCl_2$-type regions, all in-between layers contained Mg-atoms, being about half-occupied, and where these positively charged Mg^{2+}-ions tried to stay far away from each other on average, leading to a slightly disordered $CaCl_2$-type structure, but which would still be recognized in an X-ray pattern as $CaCl_2$. Since the two modifications shared all the densely packed F-atom sheets throughout the film, the presence of the small CdI_2-type nuclei stabilized the - by themselves unstable - $CaCl_2$-type regions, because they prevented the execution of shearing motion (with zero activation energy required) that otherwise transforms the $CaCl_2$-type structure to the rutile-type structure without requiring any barrier crossings.

Continuing the tempering for very long times, the CdI_2-type regions vanished due to the effective diffusion of some of the Mg-atoms into the "open" empty zones between the individual CdI_2-type layers. We note here that the presence of the $CaCl_2$-type phase prevented the CdI_2-type "FMgF-monolayers" to move towards each other along the c-axis, which usually closes the gap between these layers and thus helps stabilize the CdI_2-type structure due to a gain of van-der-Waals energy. Therefore, it was comparatively easy for the Mg-atoms to enter the region between the "monolayers" thus leading to a relatively fast destabilization of the regions exhibiting the CdI_2-type phase. But once these stabilizing CdI_2-type regions had vanished, no barriers existed that prevented a shearing motion, and the remaining (mostly) pure $CaCl_2$-type regions right away transformed into the stable rutile modification throughout the simulated MgF_2 film.

Thus, the theoretical modeling and simulation not only reproduced the experimental results of the various stages of the deposition-tempering process of the thin films of MgF_2 but also were able to explain, on the atomic level, the existence of an, in principle, kinetically unstable phase via the presence of a second - invisible to simple X-ray measurements - modification. Clearly, the simple picture of spatially separated nuclei of various modifications that compete on purely thermodynamic grounds in an effective negative pressure environment is too simple, and one needs to take the interactions among the different kinds of nuclei into account.

3.6. Phase formation in thin films of gallium as a function of deposition temperature and phase transformations during heating and cooling cycles

In the next example, the focus is on the experiment, where even in a supposedly well-known system, elemental gallium, new (meta)stable phases can appear. At standard pressure, four modifications of gallium are known in the literature [61]: the, presumably, thermodynamically stable α-Ga phase, whose density is even lower than the density of the melt, and β-, γ- and δ-Ga phases (ranked by order of energy, according to ab initio calculations, $E_\alpha < E_\beta < E_\gamma < E_\delta$), where the three metastable phases all have a higher density than the melt: $\rho_\alpha < \rho_{melt} < \rho_\gamma <\approx \rho_\beta <\approx \rho_\delta$.

These phases can be reached, more or less reproducibly, by rapid quenches from the melt (β,γ,δ) or via heterogeneous nucleation (α) from the melt, respectively. However, no direct transformations from the metastable modifications to the α-phase are observed. In order to gain more insight into the energy landscape of the gallium system, the femtosecond pulsed-laser-deposition (PLD) method [31] was employed to generate thin Ga films for many deposition temperatures (-190 °C ≤ T_D ≤ +25 °C),[62] the highest T_D being just below the melting point of gallium, +29.8 °C. [63] The stability ranges and the phase transitions of the initially obtained gallium allotropes were in-situ investigated during subsequent cooling and heating cycles over the same temperature range from -190 °C to +25 °C.). [62] (see Figure 6).

For the lowest deposition temperatures (-190 °C to -80 °C), the deposited films show the α-phase. Between -60 °C and -40 °C, the β-phase was observed, while between -40 °C and -20 °C, the γ-phase formed, and above -20 °C to room temperature amorphous films were obtained. Again, the modification with the lowest density (α-Ga) formed at the lowest deposition temperatures where the density of the deposit was even lower than the density of the melt. However, since this phase is the thermodynamically stable one, none of the other modifications appeared when tempering the α-phase at temperatures up to +25 °C. Similarly, the "high-density" phases, β– and γ–Ga, appeared at higher deposition temperatures than the low-density α-phase. This behavior appears to correlate with the expected density of the deposited films, which presumably is larger for higher deposition temperatures. Furthermore, upon tempering at somewhat higher temperatures (> -40 °C), the γ-phase transforms into the β-phase, as one might expect. However, even when tempering the β-phase at temperatures up to +25 °C, we never observe a transformation to the α-modification. Instead, a solid amorphous phase appears, which resembles a quenched super-cooled melt of liquid Ga, with a density in-between the one of the melt and the one of the β-modification.

The reason for this difficulty in reaching the α-phase is the great difference in density between the α- and the β-modifications, such that the thermodynamic fluctuation needed to generate a stable nucleus of the α-phase of critical size inside the β-phase or even inside the amorphous phase is extremely unlikely. On the other hand, the energy landscape accessible to the system when starting from the β-modification slightly below the thermodynamic melting temperature of gallium (i.e., the one defined by thermodynamic equilibrium between the α-phase and the liquid Ga-phase), is highly complex, with a multitude of accessible local minima that exhibit structural similarities to the pure β-modification and the "quenched" melt-like phase.

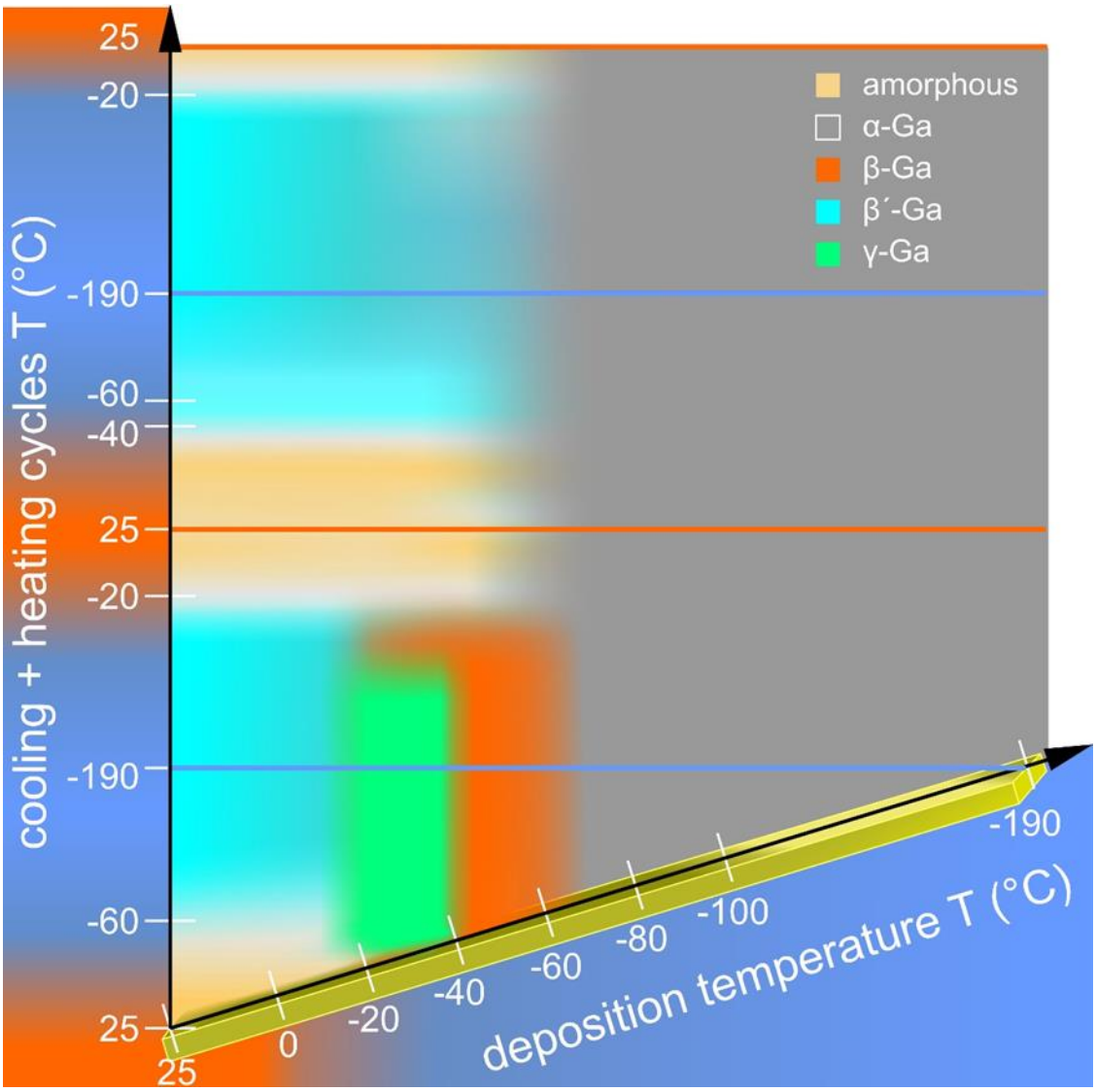

Figure 6. Deposition-temperature-annealing-schedule phase diagram, summarizing the allotropes formed during the pure gallium deposition (x-axis), followed by the phase evolution of the gallium deposits through the cooling+heating cycles (y-axis). The stability ranges of the allotropes are extrapolated from the experimental data.

This has a fascinating consequence: when cooling the system in its amorphous phase down to temperatures around -40 °C we reproducibly obtain not the β-modification, but a structurally related yet distinct new phase, which we have denoted as the β'-phase. The density of this β'-phase is larger than the one of the β-phase, and this β'-modification is preserved down to the lowest temperatures studied (-190 °C). Upon heating the β'-phase to +25 °C, we again obtain the amorphous gallium phase, from which we reproducibly regain the β'-phase upon cooling. Again, we never observe a transition from either the β'-phase or the amorphous phase to the α-modification even after long annealing cycles. Again, this is connected to the difference in the density; if we add the β'-phase and the amorphous phase to the list of densities, we obtain $\rho_{\alpha} < \rho_{melt} < \rho_{highT\text{-}amorph} < \rho_{\gamma} <\approx \rho_{\beta} <\approx \rho_{\delta} < \rho_{\beta'}$; i.e., there is a sizeable gap in density between the α-phase and both the amorphous and the β'-phase. In this context, one should also note that for depositions of Ga atoms at temperatures below liquid nitrogen temperature, e.g., at liquid He temperature, one obtains a second amorphous phase,[64] whose density $\rho_{lowT\text{-}amorph}$ should be comparable or even lower than the one of α-Ga, $\rho_{lowT\text{-}amorph} <\approx \rho_{\alpha}$,

and which would quickly evolve into the α-modification upon heating to liquid nitrogen temperature and above.

On the other hand, the α-phase remains unchanged over many heating and cooling cycles between -190 °C and +25 °C. However, we note that we observe some slight variations in the structure of the α-modification depending on the deposition temperature, which can be recognized in the relative arrangements of the (distorted) Ga-hexagons that characterize the α-Ga structure.

Ab initio calculations on various levels of refinement [65] indicate a close competition in the energy ranking among the α-, β- and β'-modifications, with the most sophisticated methods that include d-electrons and a large basis set suggesting that $E_\alpha < E_\beta < E_{\beta'}$. We also note that the simple structure suggested based on the X-ray powder data for the β'-modification might actually be an average over a multitude of structurally closely related local minima on the energy landscape inside the large multi-minima mega-basin that contains the original β-modification and many slightly different alternative structures of very similar energy (c.f. supplementary information in [62]).

From the point of view of the energy landscape of the gallium system, the stability of the β'-modification is not so much due to high-energy barriers that prevent the transformation of one unit cell of the β'-phase into a similar size unit cell of the β-phase, which is the situation one often finds in crystalline systems and is reflected in standard tree graph models of the energy landscape of crystal-forming compounds. Instead, we are dealing with a combination of entropic barriers separating the different sub-regions of the megabasin containing both the β- and β'-phases, which greatly slow down the transformation kinetics - similar to the aging kinetics in glasses mentioned earlier -, and of an entropic stabilization on the thermodynamic level due to the great malleability of the structural motifs in the β'-structure resulting in many distinct but structurally related local minima with similar energy. This is reminiscent of the currently very popular so-called high-entropy materials [66,67], where a large configurational entropy, often due to a solid solution kind of behavior, is observed to stabilize the multi-minima compound.

Besides demonstrating the importance of synthesis routes in accessing different phases of a chemical system in a reproducible manner, the example highlights the necessity of trying to explore the energy landscape of a chemical system as fully as possible not only theoretically but also experimentally, in order to get a complete overview over the structures and their stability for the many feasible modifications that are (meta)stable on physically and technically relevant time scales.

3.7. Structural details of films of ZnO as a function of the deposition temperature

The final example again demonstrates the great variety in the results of a synthesis of thin films as a function of the synthesis parameters. The system chosen, ZnO, is well-known and is employed in many technological applications, but the real material exhibits some curious properties that do not appear to be consistent with the pure ZnO compound with the ideal wurtzite structure and a clean band gap of ca. 3.4 eV [68]: essentially all crystals of ZnO are transparent, as expected, but with a (mostly) yellow color, [69] and they exhibit an intrinsic n-type conductivity [70]. In the literature, these phenomena are commonly attributed to the presence of impurities that are supposed to cause resonances in the yellow or green band and serve as the origin of impurity bands in the band structure that are then associated with the n-type conductivity.[71] Furthermore, the Raman spectra show bands at high wavenumbers, which are ascribed to the combination/overtones of some first-order Raman bands.[72]

However, these explanations are rather unsatisfying in their non-specificity and generality. Especially with regard to the Raman band at ca. 1140 cm^{-1}, assigned as multi-phonon modes derivatives from the predicted LO bands, one notes that this band is visible even if the corresponding first-order LO-bands are missing! Furthermore, they imply that essentially all samples of ZnO are not pure, and raise the question of whether the various synthesis methods employed are suitable to create pure ZnO. Thus, we have decided to generate ZnO in the form of thin films employing the femtosecond PLD method.[73,74] We are using laser ablation of a pressed, pure powder of ZnO to

create the gas phase that is deposited on a sapphire substrate, where we vary the deposition temperature from -240 °C to +300 °C. This ensures that the spurious inclusion of impurities is eliminated as much as possible.

At very low deposition temperatures, we observe a transparent colorless film of ZnO, and similar films are found at high deposition temperatures. However, at intermediate deposition temperatures, we find yellow, greyish, and opaque films. At the same time, Raman spectra of these films exhibit noticeable peaks beyond 800 cm^{-1} wavenumbers [73]. These bands fit perfectly well with the bands associated with various dioxygen species (O_2, O_2^-, O_2^{2-}). We next note that these species fit perfectly into the trigonal bipyramids formed by the Zn-sub-lattice of the ideal wurtzite structure. Usually, these bipyramids are visualized as two face-connected tetrahedra present in the hcp arrangement of the Zn-atoms, where only half of the tetrahedra are occupied by the O^{2-}-ions in the ideal wurtzite structure (c.f. Figure 7). Thus, in the ideal wurtzite crystal, all the normally filled Zn-tetrahedra are only connected via corners, with no face connection being present.

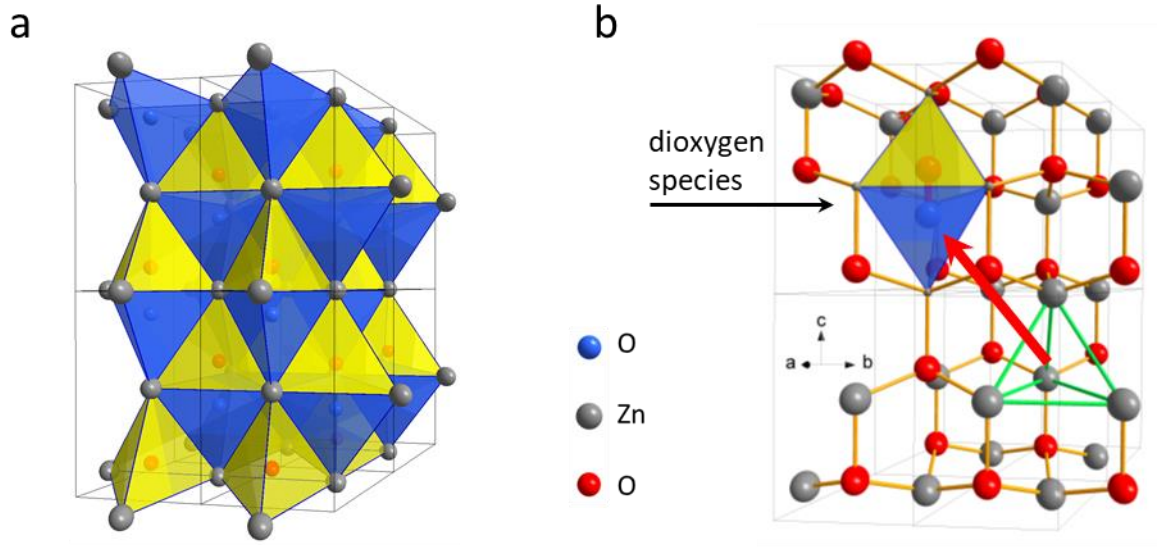

Figure 7. a) ZnO wurtzite structure (2x2x2 supercell) highlighting the OZn_4 tetrahedra arrangement, yellow tetrahedra with the tip pointing up along the c-axis (normally filled in ideal ZnO), and blue tetrahedra with tip down along the c-axis (normally empty). b) Structural realization of possible disorder in the ZnO wurtzite structure (2x2x2 supercell, distortions neglected) where one oxygen atom has moved: The figure depicts an occupied inverse tetrahedron (blue) adjacent to a filled regular tetrahedron (yellow), forming a dioxygen species, e.g., a superoxide ion (red bond); in addition, the empty (normally filled, yellow) Zn_4-tetrahedron (void) is shown by green lines.

However, during the deposition and tempering of the film, it is very easy to fill, once in a while, a tetrahedron of the orientation opposite to the normally filled Zn-tetrahedra, which results in a dioxygen species; of course, this implies that an empty Zn tetrahedron is also generated. The presence of such a filled "inverse oriented" tetrahedron is not detectable via, e.g., additional X-ray reflections. Instead, we obtain indirect evidence when analyzing the electron density derived from the diffraction patterns.[74] Here, the presence of additional occupants of the tetrahedra makes itself felt in a large broadening of the difference in electron density in the oxygen positions compared to what we would expect from an ideal ZnO wurtzite structure.

A fascinating consequence of such rearrangements of the oxygen atoms in the wurtzite structure during the film growth is the fact that the Zn-atoms no longer need to be all in the Zn^{2+} oxidation state. The formation of superoxide ions generates excess electrons ($2\ O^{2-} \rightarrow (O_2)^- + 3\ e^-$). It follows that there are additional "free" electrons in the structure, which account for the intrinsic n-type conductivity. Furthermore, in the intermediate range of deposition temperatures, the local depletion of the Zn tetrahedra is quite concentrated in nanometer-sized regions, and X-ray reflections typical of

metallic zinc are present in the diffraction pattern, where the width of the peaks indicates that the size of these Zn metal regions is in the nanometer range. From this, one concludes that mesoscopic regions of metallic zinc are formed throughout the film at intermediate temperatures, whose existence is further supported by the greyish color of the films. In addition, we note that the yellowish tinge is caused by the yellow superoxide ion O_2^- present in the film.

This example demonstrates, how the systematic use of special synthesis methods can result in different compounds or variations of a given compound represented on the energy landscape of the ZnO system, ranging from the pure wurtzite ZnO to a combination of Zn metal and ZnO, including the presence of superoxide ions.

Still, perhaps more important than the variability of synthesis outcomes even for pure systems of a well-defined overall composition, ZnO, this example system highlights our general underappreciation of the structural and compositional flexibility of supposedly simple, even binary, ceramic-type compounds; in alloys such flexibility is well-recognized, of course. This is going to be an even more relevant issue in the future since such detailed knowledge of the structural variability of a compound will become more and more crucial as we try to control a system's properties on smaller length scales down to the atomic level. Furthermore, when we try to employ such materials, we need to be able to establish time scales for the stability of the metastable modifications of the compounds of interest, which includes detailed information about the pathways for their decay or transformation to other (meta)stable or intermediary modifications. Clearly, the degree of control we have over such a material that is tuned and exploited down to the atomic level greatly relies on the completeness of our structural knowledge about the system.

4. Discussion and conclusions

In the preceding section, we have considered several examples of thin films and monolayers, the interplay of theory and experiment - including chemical synthesis and in-situ physical measurements - concerning the prediction of possible modifications and their structures, and demonstrated the influence of the synthesis parameters and subsequent treatment of a deposited film on the formation of additional modifications, the transformations between modifications and their properties. Furthermore, we have highlighted the importance of using such tools for the analysis of the whole field of possible stable and metastable phases that exist on the energy landscape of the chemical system, and for elucidating the structural basis of unusual physical properties.

All this work can be seen as contributing to the field of systematic synthesis exploration in a chemical system, which encompasses the theoretical prediction of synthesis targets via the study of the energy landscapes of a chemical system, the simulation of synthesis routes that are employed in attempts to reach such targets in the experiment, and finally the careful reproducible performance of such syntheses on well-defined chemical systems, where the syntheses are accompanied by, e.g., X-ray, IR, Raman or other measurements that yield structural data about the current state of the system at all stages of the syntheses and subsequent transformations of the material. The long-term goal of this joined theoretical and experimental enterprise is to achieve such a high degree of control in the experiment, that we are able to reach all regions of the energy landscape not only in the computer but also in the experiment - in some ways this can be understood as the final aim and highest possible achievement of the field of solid state chemistry.[15]

In particular in the field of thin films and monolayers which are essentially two-dimensional and thus allow us much more access than a bulk 3D system, such a control should, in principle, be feasible on the atomic level. In the ideal case, one would place the atoms or molecules one-by-one on a smooth surface, next to and on top of one another, at extremely low temperatures, such that their arrangement is as close as possible to one of the metastable structural arrangements we have found on the energy landscape. Activating the formation of bonding by adding heat or radiation, we could thus realize essentially all metastable modifications of the chemical system.

In the examples presented above, the starting point of the growth of the monolayers of molecules (c.f. sections 3.2 and 3.3) were individual molecules that were deposited on the surfaces and then rearranged themselves into islands with common (periodic) structural features or reacted to

form an amorphous layer. These structures corresponded to typical local minimum structures found during global optimizations or molecular dynamics simulations of the monolayers. We note that the periodic islands seen in the experiment exhibited one of the many possible very similar dense periodic packings of the molecules with similar energies found on the energy landscape. This is a typical problem with molecular crystals, where the energy differences between many similar arrangements are so small that the quality of the energy function is not always sufficient to establish the correct energy ranking among the local minima needed to identify the true global minimum. [75,76] Similarly, the amorphous arrangement was not the global minimum, which was a perfect periodic hexagonal arrangement of the reacted precursor molecules, according to the simulations; since in this case chemical bonds were involved as the major stabilizing force of the possible structures, the theoretical prediction of the global minimum is more reliable than in the case of a molecular packing controlled by van-der-Waals and hydrogen-bond interactions.

In contrast, for the thin films grown from the gas phase (3.4 - 3.7), the constituents of the entities that were to be deposited on a substrate were generated by global, i.e., thermal, or local, i.e., via laser ablation, heating of a solid compound with the same composition as the final product of interest. As a consequence, the gas phase before deposition consisted of various small or larger clusters or molecules with essentially the same composition as the source material; in particular, we note that in these fragments the various atoms already have neighbor atoms in similar numbers as in the source material, although the detailed structure of small clusters usually is quite different from cut-outs of the bulk crystal. This fact clearly might prejudice the resulting deposit when these clusters reach the surface and form the thin (amorphous) film at low temperatures, thus locking the system into a small region of the energy landscape. In some fashion, this method is reminiscent of the classical gas phase transport synthesis method [77] for the synthesis of out-of-equilibrium solids starting from a stable modification of the compound.

Such a lock-in can be possibly avoided by synthesizing the thin film directly from the individual elements, ideally in the form of single atoms being deposited on the substrate, usually at random unless STM/AFM or related techniques are available that allow a single atom placement on a given surface; however, the latter are not yet ready for macroscopic thin film production. For such a separate-atom deposition procedure, multiple evaporation and/or plasma sources are needed, one for each type of atom involved in the system. Only a few studies have been performed in this fashion, most notably the synthesis of the two metastable nitrides Na_3N [33] and K_3N [78] about twenty years ago.

However, in contrast to the deposition of the fragments with well-defined ratios of the different atom types involved, we need to fine-tune the strength of the various sources, in order to achieve a certain desired composition of the initial deposit. On the one hand, this is a serious complication of the synthesis method, since it is nearly impossible to guarantee that what arrives on the substrate exhibits exactly the target composition. On the other hand, by employing a narrow mesh of evaporation parameters, we can scan a large range of compositions in the thin films we generate, even for binary, and much more so for ternary or higher-order compounds of interest. We already have seen in the example of LiBr, how the control of the evaporation rate, i.e., of the gas phase pressure, allowed us to identify the exact range of deposition temperature-vapor pressure combinations that yielded the desired metastable LiBr modification. Thus, controlling the composition of an atom-level mixed deposit at low temperatures via small variations of the source parameters, allows us, in principle, to scan the whole phase spectrum of a chemical system, including not only thermodynamically stable but also metastable phases as a function of composition and deposition and process temperatures. Of course, this requires a large effort, ideally performed with modern robotic assistant high-throughput techniques employing multiple synthesis chambers at the same time. But once enough information has been accumulated about a given chemical system or many related ones, this can be fed into modern machine learning neural networks, with the goal to be able to obtain fast suggestions of optimal control parameters for the sources and other synthesis parameters when targeting a certain kind of metastable phase in a given chemical system. Similarly, the analysis of, e.g., the thousands of X-ray patterns produced by a high-throughput experiment that had been performed by hand in the past, can be assisted by an automated (pre-)screening in the future, using (self-learning) neural network based pattern recognition and pattern learning systems.

To demonstrate the power of the atom-separated deposition approach even without the high-throughput machinery, we want to discuss some curious features of two other examples that have been investigated using separate sources for each atom type: the synthesis of $AgNO_3$ films [32] from Ag, N and O atoms deposited at random on a sapphire substrate, and a study of the Mg/N system [79], where the ratio between Mg and N atoms was systematically varied during the deposition.

In the case of the Ag/N/O system, silver was deposited together with plasma-activated nitrogen and oxygen in approximately the ratio of N:O = 1:3 at -180 °C, and while the material was slowly heated up to +130 °C, powder patterns were acquired at a number of intermediary temperatures. At the lowest temperatures up to ca. -150 °C, only a broad amorphous hump could be seen, indicating that the deposit was still in the amorphous state. At -110 °C, we observe first reflections indicating the formation of a crystalline phase, but this phase corresponds to the molecular crystal of N_2O_4, with the silver in the system still being in the amorphous state. Here, we note that we are already close to the temperature range where the N_2O_4 molecular crystal begins to evaporate.[32,80]

But once we reach -70 °C, the X-ray reflections indicating the N_2O_4 molecular crystals vanish, and are replaced by a set corresponding to the high-temperature phase of $AgNO_3$, which remains present up to room temperature (even though HT-$AgNO_3$ is metastable at these low temperatures). Sometimes small impurities of AgO were also detected as a byproduct. While this outcome was unexpected at the time of the experiment, this is no real surprise, since the density of the amorphous material is lower than the one of the HT-$AgNO_3$ modification which in turn is lower than the one of the low-temperature modification of $AgNO_3$, and thus the nuclei of the high-temperature phase are enthalpically preferred over those of the low-temperature phase inside the amorphous matrix. When increasing the temperature to 85 °C, the compound transforms into the thermodynamically stable low-temperature modification LT-$AgNO_3$, and at even higher temperatures, we recover the - by now thermodynamically stable - HT-$AgNO_3$ phase.[32,80]

While this sequence of amorphous, HT-, LT- and again HT-phases of $AgNO_3$ with increasing temperature is quite fascinating in its own right, perhaps the most thought-provoking aspect is the observation that inside the semi-amorphous film the same kind of chemical reaction appears to take place, which occurs in the standard aqueous solution chemistry ($Ag + HNO_3(aq) \rightarrow AgNO_3(aq)$), under seemingly completely different circumstances. Seen from the point of view of time scales, we realize that the atom-level mixing present in the amorphous thin film allows chemical processes to take place at experimental time scales, which are completely analogous to the fast processes in melts or aqueous solutions that are enabled by the fast diffusion of the reaction participants in the melt or solution.

In this context, we note that when we repeat the same procedure by replacing Ag with Au in the deposition process, the N_2O_4 crystals form already at the lowest temperature (-180 °C), which indicates that no strong Au-O bonds are formed that would compete with the crystallization of N_2O_4. Upon heating the sample, the N_2O_4 crystals again vanish at around -100 °C, but instead of $AuNO_3$, we now find only tiny crystalline gold particles (with a diameter of only a few dozen nanometers, based on the width of the diffraction peaks), again in agreement with the solution chemistry experiments where Au does not dissolve in nitric acid.[80]

Similarly, the study of the Mg/N system with a wide variation of compositions deposited at room temperature (T_D = +25 °C) from atom-type separated sources, resulted in the formation of unusual phases as a function of source parameters and annealing temperature. If we consider the powder patterns of a sample prepared employing an intermediate rate of Mg deposition (Mg source at 320 °C, nitrogen flux of 1.5 cm^3/min activated by a 80 mA microwave-plasma) at room temperature, we observe the reflections of a fcc-atom arrangement of the Mg atoms (called β-Mg), the presence of which is supported by corresponding Rietveld refinements (Fm-3m, a=451.6 pm) and XPS studies. In contrast, after annealing up to 300 °C the reflections correspond to a mixture of the standard hcp-packing of Mg atoms (α-Mg) and the crystalline Mg_3N_2 compound. We note that the first reflections characteristic of crystalline Mg_3N_2 begin to be observed already at around +200 °C, together with clear peaks belonging to the β-Mg modification, while the presence of crystalline α-Mg is only confirmed at around +300 °C where no peaks of β-Mg remain. It appears that when the amorphous Mg/N matrix is transformed into crystallized Mg_3N_2, β-Mg loses its stability and transforms into the

global minimum α-Mg on the energy landscape of magnesium. We recall (see section 3.5) the case of the unstable, in principle, $CaCl_2$ phase in the thin films of MgF_2, which was stabilized by the presence of essentially invisible nanometer-size crystals of the metastable CdI_2 modification, where the $CaCl_2$ phase transformed, without requiring activation energy, into the stable rutile modification once the CdI_2 phase had vanished.

Regarding the outcome for different deposition rates of magnesium, we find that if the Mg rate is reduced (Mg source running at 300 °C) only Mg_3N_2 is formed on the substrate and if the Mg rate is increased (Mg source at 340 °C) then a mixture of Mg_3N_2, β-Mg, and α-Mg is obtained. Thus, with increasing Mg content the reaction of magnesium and nitrogen reaches a point where only a part of Mg reacts to magnesium nitride, and thus first β-Mg and later α-Mg remains as a byproduct. If we now vary the parameters of the plasma source (while keeping the Mg source at 320 °C), we find that as long as we supply a high activation of nitrogen atoms, the β-phase of Mg is present, possibly together with some crystals of Mg_3N_2. However, when we reduce the activation of nitrogen, we only obtain pure α-Mg, which clearly indicates that the presence of some additional amorphous Mg/N phase is needed for the stabilization of β-Mg. In this context, we note that β-Mg would be kinetically stable against the transformation into α-Mg, at least at low temperatures, since it constitutes a low-energy local minimum on the energy landscape of elementary Mg, in contrast to the $CaCl_2$ structure in the MgF_2 system, which does not correspond to a local minimum on the landscape of MgF_2.

These two short examples display not only the richness of the landscape of the chemical system investigated, but also the subtle features of the synthesis in the solid state, and how even small changes in synthesis and processing conditions can stabilize or destabilize the many competing metastable phases in the system. Together with the examples discussed in more detail in section 3, which have demonstrated the strength of combining theory and experiment in the realization and analysis of metastable compounds, these studies and their surprising results also highlight the many gaping holes in our understanding of chemical systems, e.g., why does β-Mg seem to require the presence of amorphous Mg_2N_3 for its stabilization, or why does the aqueous solution reaction that produces $AgNO_3$ take place in a seemingly analogous fashion in the solid film?

Although the aim of developing a rational approach to the planning of solid-state syntheses in analogy to the toolbox of organic chemistry was formulated already in the 1990s [81] and discussed as a vision even earlier [82], it often feels as if we were still at the beginning. The past three decades have seen much progress in the field of structure prediction of crystalline modifications [11,83], and the concept of the energy landscape of a chemical system as the world where the chemistry of a material takes place is by now well-established among theorists and experimentalists [11,84] Nevertheless, in the field of solid-state chemistry, the focus still appears to remain on the ideal crystal structure, and the path to the synthesis of such ideal modifications is chosen by analogy to successful syntheses in similar systems. But the examples discussed here in the context of low-dimensional materials clearly show that one needs to explore the whole energy landscape of the chemical system, including the complex barrier structure that lies beyond the singular local minima that correspond to the ideal crystals, from both a theoretical and experimental point of view. In reality, we never obtain such an ideal flawless arrangement of atoms, neither in the experiment nor during a molecular dynamics simulation containing a sufficiently large number of atoms to represent a real macroscopic system (unless we start with the ideal structure and stay at very low temperatures). Instead, in both the experiments and the simulations, we explore the landscape's mega basins or locally ergodic regions, each of which contains the many minima associated with defect structures that together represent the real crystals for each given crystalline phase. Furthermore, we need to identify the true pathways the system follows during synthesis and transformation processes for given external boundary conditions (temperature, pressure, etc.), both in the experiment and on a theoretical level. But this means, we must not only study the successful routes but also learn about the dead-ends, learn to understand why they are "failures", and how we can exert control over the path the system takes on the landscape according to the laws of physics. From a theoretical point of view, this means that it is not sufficient to study the energy landscape of the isolated chemical system, but we also need to investigate the landscape of the system in contact with the environment. This includes not only variations in the thermodynamic boundary conditions such as temperature, pressure, electromagnetic fields, etc., but also the presence of atoms belonging to a substrate, a solution, or a melt that serve as surface or

medium, respectively, where the synthesis takes place.[11,85] Dealing with these influences via modeling and simulations is a tremendous challenge, of course. Both the sheer number and diversity of the atoms involved and the large time scales of the chemical processes during the synthesis push the boundaries of the feasible as far as computational resources are concerned, in particular since the simulations should take place on an ab initio level wherever possible. Nevertheless, great progress has been made in recent years, both regarding the development of faster algorithms and with respect to suitable energy functions, where the use of machine-learning for accelerating the computation of ab initio energies and forces is a highly active field[86] although surely no panacea.

Once we have gained such an understanding, we can complement the atom level description by an appropriate and useful continuum description of the chemical system, for which phenomenological models describing various combinations of reaction-, diffusion-, growth-, etc. processes can be formulated with spatio-temporal resolution. To achieve this, both theory and experiment have to contribute: the theorist by studying the landscape of the system for substantial numbers of atoms, in order to acquire some realism as far as the atom level processes are concerned, while the experimentalist needs to carefully analyze the seemingly uninteresting results of his syntheses as these also tell us important information about the chemistry, i.e., the structural and compositional changes, in a material.

Together, they can open up a comprehensive view of the whole chemical system, and the surprising richness of the chemistry in even those systems that are often declared "dead" and uninteresting. Once such a full understanding has been achieved, the road is open to the systematic generation of new materials for future technological applications.

References:

[1] R. Arroyave, D. L. McDowell: Systems Approaches to Materials Design: Past, Present, and Future, Annu. Rev. Mater. Res., (2019), 49, 103-126.
[2] D. Banerjee: Towards a Sustainable Future with Materials, J. Ind. Inst. Sci., (2022), 102, 5-9.
[3] C. N. R. Rao, H.S.S. Ramakrishna, U. Maitra: Graphene Analogous of Inorganic Layered Materials, Angew. Chem. Int. Ed., (2013), 52, 13162-13185.
[4] W. Zhang, H. Li, E. Hopmann, A. Y. Elezzabi: Nanostructured inorganic electrochromic materials for light applications, Nanophotonics, (2021), 10, 825-850.
[5] X. Titan, Y. Zhang, R. Zheng, D. Wei, J. Liu: Two-dimensional organic-inorganic hybrid Ruddlesden-Popper perovskite materials: preparation, enhanced stability, and applications in photodetection, Sustainable Energy Fuels, (2020), 4, 2087-2113.
[6] A. Gutiérrez-Cruz, A. R. Ruiz-Hernández, J. F. Vega-Clemente, et al.: A review of top-down and bottom-up synthesis methods for the production of graphene, graphene oxide and reduced graphene oxide, J. Mater. Sci., (2022), 57, 14543–14578.
[7] M. Li, L. Li, Y. Fan, F. Jiao, D. Geng, W. Hu: From top to down – Recent advances in etching of 2D materials, Adv. Mater. Interfaces, (2022), 9, 2201334.
[8] H. Zheng, S. Ravaine: Bottom-up assembly and applications of photonic materials, Crystal, (2016), 6, 54.
[9] K. Ariga, J. P. Hill, Q. Ji: Layer-by-layer assembly as a versatile bottom-up nanofabrication technique for exploratory research and realistic application, Phys. Chem. Chem. Phys., (2007), 9, 2319-2340.
[10] J. C. Schön: Nanomaterials - What energy landscapes can tell us, Proc. Appl. Ceram., (2015), 9, 157-168
[11] J. C. Schön: Energy landscapes in inorganic chemistry, in Comprehensive Inorganic Chemistry III, eds. J. Reedijk, K. Poeppelmeier (Elsevier, Amsterdam, 2023), Chapter 127 (3.11), 262-392; DOI: 10.1016/B978-0-12-823144-9.00127-8
[12] R. Ferrando, J. Jellinek, R. L. Johnston: Nanoalloys: From Theory to Applications of Alloy Clusters and Nanoparticles, Chem. Rev., (2008), 108, 845-910
[13] D. H. Bowskill, I. J. Sugden, S. Konstantinopoulos, C. S. Adjiman, C. C. Pantelides: Crystal Structure Prediction Methods for Organic Molecules: State of the Art, Annu. Rev. Chem. Biomol. Eng., (2021), 12, 593-623
[14] J. C. Schön: Structure prediction in low dimensions - concepts, issues and examples, Phil. Trans. Roy. Soc. A, (2023), 381, 20220246
[15] J. C. Schön: On the way to a theory of solid state synthesis: Issues and open questions, Adv. Chem. Phys., (2015), 157, 125-134
[16] J. C. Schön: Finite-Time Thermodynamics and the Optimal Control of Chemical Syntheses, Z. Anorg. Allg. Chem., (2009), 635, 1794-1806
[17] K. H. Hoffmann, J. C. Schön: Controlled dynamics on energy landscapes, Eur. Phys. J. B, (2013), 86, 220_1-10
[18] K. H. Hoffmann, J. C. Schön: Combining pressure and temperature control in dynamics on energy landscapes, Eur. Phys. J. B, (2017), 90, 84
[19] F. Musil, S. De, J. Yang, J. E. Campbell, G. M. Day, M. Ceriotti: Machine learning for the structure-energy-property landscapes of molecular crystals, Chem. Sci., (2018), 9, 1289-1300
[20] J. Wei, X. Chu, X.-Y. Sun, K. Xu, H.-X. Deng, J. Chen, Z. Wei, M. Lei, Machine learning in materials science, InfoMat, (2019), 1, 338-358
[21] H. Ünlü, N. J. M. Horing, Eds.: Progress in Nanoscale and Low-Dimensional Materials and Devices: Properties, Synthesis, Characterization, Modelling and Applications, (SpringerNature, Cham, 2022)
[22] P. Miro, M. Audiffred, T. Heine: An atlas of two-dimensional materials, Chem. Soc. Rev. (2014), 43, 6537-6554
[23] S. Kirkpatrick, C. D. Gelatt, Jr., M. P. Vecchi: Optimization by Simulated Annealing, Science, (1983), 220, 671-680
[24] J. C. Schön: Studying the Energy Hypersurface of Multi-Minima Systems - the Threshold and the Lid Algorithm, Ber. Bunsenges., (1996), 100, 1388 - 1391

[25] S. Neelamraju, C. Oligschleger, J. C. Schön: The threshold algorithm: Description of the methodology and new developments, J. Chem. Phys., (2017), 147, 152713
[26] S. Neelamraju, R. L. Johnston, J. C. Schön: A threshold-minimization scheme for exploring the energy landscape of biomolecules: Application to a cyclic peptide and a disaccharide, J. Chem. Theo. Comp., (2016), 12, 2471-2479
[27] W. Margerit, A. Charpetier, C. Maugis-Rabusseau, J. C. Schön, N. Tarrat, J. Cortes: IGLOO: an Iterative Global exploration and LOcal Optimization algorithm to find diverse low-energy conformations of flexible molecules, submitted to "Algorithms", (2023)
[28] N. Metropolis and A. W. Rosenbluth and M. N. Rosenbluth and A. H. Teller and E. Teller: Equation of State Calculations by Fast Computing Machines, J. Chem. Phys., (1953), 21, 1087-1092
[29] Z. Ouyang, Z. Takats, T. A. Blake, B. Gologan, A. J. Guymon, J. M. Wiseman, J. C. Oliver, V. J. Davisson, R. G. Cooks: Preparing Protein Microarrays by Soft-Landing of Mass-Selected Ions, Science, (2003), 301, 1351-1354
[30] D. Fischer, A. Müller, M. Jansen: Existiert eine Wurtzit-Modifikation von Lithiumbromid? - Untersuchungen im System LiBr/LiI -, Z. Anorg. Allg. Chem., (2004), 630, 2697-2700.
[31] D. Fischer, L. V. Meyer, M. Jansen, K. Müller-Buschbaum: Highly Luminescent Thin Films of the Dense Framework [$EuIm_2$] with Switchable Transparency Formed by Scanning Femtosecond-Pulse Laser Deposition, Angew. Chem. Int. Ed., (2014), 53, 706-710.
[32] D. Fischer, M. Jansen: Low-Activation Solid-State Syntheses by Reducing Transport Lengths to Atomic Scales as Demonstrated by Case Studies on $AgNO_3$ and AgO, J. Am. Chem. Soc., (2002), 124, 3488-3489
[33] D. Fischer, M. Jansen: Synthesis and Structure of Na_3N, Angew. Chem. Int. Ed., (2002), 41, 1755-1756
[34] R. Gutzler, J. C. Schön: Two-dimensional Silicon-Carbon Compounds: Structure Prediction and Band Structures, Z. Anorg. Allg. Chem., (2017), 643, 1368-1373
[35] C. M. Polley, H. Fedderwitz, T. Balasubramanian, A. A. Zakharov, R. Yakimova, O. Bäcke, J. Ekman, S. P. Dash, S. Kubatkin, S. Lara-Avila: Bottom-Up Growth of Monolayer Honeycomb SiC, Phys, Rev. Lett., (2023), 130, 076203
[36] S. Abb, N. Tarrat, J. Cortes, B. Andriyevsky, L. Harnau, J. C. Schön, S. Rauschenbach, K. Kern: Carbohydrate Self-Assembly at Surfaces: STM Imaging of Sucrose Conformation and Ordering on Cu(100), Angew. Chem. Int. Ed., (2019), 58, 8336-8340
[37] B. Andriyevsky, N. Tarrat, J. Cortes, J. C. Schön: Dehydrogenation versus deprotonation of disaccharide moelcules in vacuum: a thorough theoretical investigation, Roy. Soc. Open Sci., (2022), 9, 220436
[38] J. C. Schön, C. Oligschleger, J. Cortes: Prediction and clarification of structures of (bio)molecules on surfaces, Z. Naturf. B, (2016), 71, 351-374
[39] S. Abb, L. Harnau, J. C. Schön, J. Cortes, S. Rauschenbach, K. Kern: Disaccharide self-assembly behavior on metal surfaces (European Conference on Surface Science-31, Barcelona, September 2015)
[40] S. Abb, N. Tarrat, J. Cortes, B. Andriyevsky, L. Harnau, J. C. Schön, S. Rauschenbach, K. Kern: Polymorphism in carbohydrate self-assembly at surfaces: STM imaging and theoretical modelling of trehalose on Cu(100), RSC Advances, (2019), 9, 35813-35819
[41] W. H. Zachariasen: The Atomic Arrangement in Glass (Continuous Random networks), J. Am. Chem. Soc., (1932), 54, 3841-3851
[42] J. Van Turnhout, P. Th. A. Klaase, P. H. Ong, L. C. E. Struik: Physical aging and electrical properties of polymers, J. Electrostat., (1977), 3, 171-179
[43] L. Lundgren, P. Svedlindh, P. Nordblad, O. Beckman: Dynamics of the relaxation time spectrum in a CuMn spin glass, Phys. Rev. Lett., (1983), 51, 911-914
[44] M. Utz, P. G. Debenedetti, F. H. Stillinger: Atomistic Simulation of Aging and Rejuvenation in Glasses, Phys. Rev. Lett., (2000), 84, 1471-1474
[45] A. Hannemann, J. C. Schön, M. Jansen, P. Sibani: Nonequilibrium Dynamics in Amorphous $Si_3B_3N_7$, J. Phys. Chem. B, (2005), 109, 11770 - 11776
[46] P. Alexa, C. Oligschleger, P. Gröger, C. Morchutt, B. Vyas, B. V. Lotsch, J. C. Schön, R. Gutzler, K. Kern: Short-Range Structural Correlations in Amorphous 2D Polymers, ChemPhysChem, (2019), 20, 2340 - 2347

[47] Z. Cancarevic: Prediction of not-yet-synthesized solids at extreme pressures, and the development of algorithms for local optimization on ab-initio level, (PhD-thesis, University of Stuttgart, 2006)
[48] Z. Cancarevic, J. C. Schön, M. Jansen: Stability of alkali metal halide polymorphs as function of pressure, Chem. Asian J., (2008), 3, 561-572
[49] Y. Liebold-Ribeiro, D. Fischer, M. Jansen: Experimental Substantiation of the "Energy Landscape Concept" for Solids: Synthesis of a New Modification of LiBr, Angew. Chem. Int. Ed., (2008), 47, 4428-4431
[50] J. C. Schön, M. Jansen: Determination of Candidate Structures for Simple Ionic Compounds through Cell Optimisation, Comp. Mater. Sci., (1995), 4, 43 - 58
[51] D. Zagorac, J. C. Schön, M. Jansen: Identification of promising chemical systems for the synthesis of new materials structure types: An ab initio minimization data mining approach, Proc. Appl. Ceram., (2012), 7, 37-41
[52] A. Bach, D. Fischer, M. Jansen: Synthesis of a New Modification of Lithium Chloride Confirming Theoretical Predictions, Z. Anorg. Allg. Chem., (2009), 635, 2406-2409
[53] A. Bach, D. Fischer, M. Jansen: Metastable Phase Formation of Indium Monochloride from an Amorphous Feedstock, Z. Anorg. Allg. Chem., (2013), 639, 465-467
[54] A. Bach, D. Fischer, X. Mu, W. Siegle, P. A. van Aken, M. Jansen: Structural Evolution of Magnesium Difluoride: from an Amorphous Deposit to a New Polymorph, Inorg. Chem., (2011), 50, 1563-1569
[55] X. Mu, S. Neelamraju, W. Sigle, C.T. Koch, N. Toto, J. C. Schön, A. Bach, D. Fischer, M. Jansen, P. A. van Aken: Evolution of order in amorphous-to-crystalline phase transformation of MgF_2, J. Appl. Cryst., (2013), 46, 1105-1116
[56] S. Neelamraju, J. C. Schön, M. Jansen: Atomistic Modeling of the Low-Temperature Atom-Beam Deposition of Magnesium Fluoride, Inorg. Chem., (2015), 54, 782-791
[57] M. A. C. Wevers, J. C. Schön, M. Jansen: Determination of structure candidates of simple crystalline AB_2-systems, J. Solid State Chem., (1998), 136, 233 - 246
[58] M. A. C. Wevers, J. C. Schön, M. Jansen: Global Aspects of the Energy Landscape of Metastable Crystal Structures in Ionic Compounds, J. Physics: Cond. Matt., (1999), 11, 6487 - 6499
[59] S. Neelamraju, J. C. Schön, K. Doll, M. Jansen: Ab initio and empirical energy landscapes of $(MgF_2)_n$ clusters (n = 3, 4), Phys. Chem. Chem. Phys., (2012), 14, 1223-1234
[60] S. Neelamraju, A. Bach, J. C. Schön, D. Fischer, M. Jansen: Experimental and theoretical study of Raman spectra of magnesium fluoride clusters, J. Chem. Phys., (2012), 137, 194319
[61] A. Defrain: Etats metastables du gallium. surfusion et polymorphisme, J. Chim. Phys. , (1977), 74, 851–62
[62] D. Fischer, B. Andriyevsky, J. C. Schön: Systematics of the allotrope formation in elemental gallium films, Mater. Res. Express, (2019), 6, 116401-1-31
[63] W.M. Haynes (Hrsg.) CRC Handbook of Chemistry and Physics 94th ed. (Boca Raton: CRC, Taylor&Francis group) 4 (2013)-121-136
[64] O. Hunderi, R. Ryberg: Amorphous gallium - a free electron metal, J. Phys. F: Met. Phys., (1974), 4, 2096-2102
[65] B. Andriyevsky, D. Fischer, J. C. Schön, (2023), unpublished
[66] M.-H. Tsai, J.-W. Yeh: High-Entropy Alloys: A Critical Review, Mater. Res. Lett., (2014), 2, 107-123
[67] E. P. George, R. O. Ritchie: High-entropy materials, MRS Bulletin, (2022), 47, 145-150
[68] H. Moroc, Ü. Özgür: Zinc oxide: Fundamentals, materials and device technology, (Wiley-VCH, Weinheim 2009), 1
[69] D. Ehrentraut, H. Sato, Y. Kagamitani, H. Sato, A. Yoshikawa, T. Fukuda: Solvothermal growth of ZnO, Prog. Crystal Growth Charact. Mater., (2006), 52, 280-335
[70] A. Wang: Electrical conductivity and doping, Springer Series in Materials Science 120 Zinc Oxide, chapter 5, (Springer, Berlin 2010), 95
[71] I. Ayoub, V. Kumar, R. Abolhassani, R. Sehgal, V. l Sharma, R. Sehgal, H. C. Swart, Y. K. Mishra: Advances in ZnO: Manipulation of defects for enhancing their technological potentials, Nanotechnol. Rev., (2022), 11, 575-619.

[72] R. Cusco, E. Alarcón-Lladó, J. Ibáñez, L. Artús, J. Jiménez, B. Wang, M. J. Callahan: Temperature dependence of Raman scattering in ZnO, Phys. Rev. B, (2007), 75, 165202
[73] D. Fischer, D. Zagorac, J. C. Schön: The presence of superoxide ions and related dioxygen species in zinc oxide - a structural characterization by in-situ Raman spectroscopy, J. Raman Spectr., (2022), 53, 2137-2146
[74] D. Fischer, D. Zagorac, J. C. Schön: Fundamental insight into the formation of the zinc oxide crystal structure, Thin Solid Films, (2023), 782, 140017
[75] X. Bidault, S. Chaudhuri: How Accurate Can Crystal Structure Predictions Be for High-Energy Molecular Crystals ?, Molecules, (2023), 28, 4471
[76] K. Kriz, L. Schmidt, A. T. Andersson, M.-M. Walz, D. van der Spoel: An Imbalance in the Force: The Need for Standardized Benchmarks for Molecular Simulation, J. Chem. Inf. Model., 2023, 63, 412-431
[77] M. Binnewies, R. Glaum, M. Schmidt, P. Schmidt: Chemical Vapor Transport Reactions, (De Gruyter, Berlin, 2012)
[78] D. Fischer, Z. Cancarevic, J. C. Schön, M. Jansen: Zur Synthese und Struktur von K_3N, Z. Anorg. Allg. Chem., (2004), 630, 160
[79] D. Fischer, M. Jansen: Does magnesium crystallize only in the Mg-type structure ? (HÄKO presentation, Regensburg, 3.3.-5.3.2005)
[80] D. Fischer: Research Report (MPI for Solid State Research, Stuttgart, 18.10.2006)
[81] J. C. Schön, M. Jansen: A first step towards planning of syntheses in solid state chemistry: determination of promising structure candidates using global optimization, Angew. Chem. Int. Ed., (1996), 35, 1286 - 1304
[82] M. Jansen: Syntheseplanung in der Festkörperchemie (Presentation at the 30th anniversary of the Fonds der Chemie, Düsseldorf, 1980)
[83] L. J. Conway, C. J. Pickard, A. Herrmann: First principles crystal structure prediction, in Comprehensive Inorganic Chemistry III, eds. J. Reedijk, K. Poeppelmeier (Elsevier, Amsterdam, 2023), Chapter 128 (3.12), 393-420
[84] A. J. Martinolich, J. R. Neilson: Pyrite Formation via Kinetic Intermediates through Low-Temperature Solid-State Metathesis, J. Am. Chem. Soc., 2014, 136, 15654-9
[85] J. C. Schön: Energy Landscape Concepts for Chemical Systems under Extreme Conditions, J. Innov. Mater. Extr. Cond., (2021), 2, 5-57
[86] F. Lu, L. Cheng, R. J. DiRisio, J.M. Finney, M. A. Boyer, P. Moonkaen, J. Sun, S. J. R. Lee, J. E. Deustua, T. F. Miller III, A. B. McCoy: Fast Near Ab Initio Potential Energy Surfaces Using Machine Learning, J. Phys. Chem. A, (2022), 126, 4013-4024